RESEARCH ARTICLE | SEPTEMBER 28 2015

Solar cells with gallium phosphide/silicon heterojunction FREE

Maxime Darnon; Renaud Varache; Médéric Descazeaux; Thomas Quinci; Mickaël Martin; Thierry Baron; Delfina Muñoz

AIP Conf. Proc. 1679, 040003 (2015)
https://doi.org/10.1063/1.4931514

Solar Cells with Gallium Phosphide / Silicon Heterojunction

Maxime Darnon[1,a)], Renaud Varache[2], Médéric Descazeaux[1,2], Thomas Quinci[1,2,3], Mickaël Martin[1], Thierry Baron[1] and Delfina Muñoz[2]

[1]*Univ. Grenoble Alpes , CNRS, CEA-Leti Minatec, LTM, F-38054 Grenoble Cedex, France*
[2]*CEA-INES, LITEN, 50 Avenue du Lac Léman, F-73375 Le Bourget-du-Lac, France*
[3]*Université Européenne de Bretagne, INSA, FOTON-OHM, F-35708 Rennes, France*

[a)]Corresponding author: maxime.darnon@usherbrooke.ca

Abstract. One of the limitations of current amorphous silicon/crystalline silicon heterojunction solar cells is electrical and optical losses in the front transparent conductive oxide and amorphous silicon layers that limit the short circuit current. We propose to grow a thin (5 to 20 nm) crystalline Gallium Phosphide (GaP) by epitaxy on silicon to form a more transparent and more conducting emitter in place of the front amorphous silicon layers. We show that a transparent conducting oxide (TCO) is still necessary to laterally collect the current with thin GaP emitter. Larger contact resistance of GaP/TCO increases the series resistance compared to amorphous silicon. With the current process, losses in the IR region associated with silicon degradation during the surface preparation preceding GaP deposition counterbalance the gain from the UV region. A first cell efficiency of 9% has been obtained on ~5x5 cm^2 polished samples.

INTRODUCTION

Highest efficiency silicon-based solar cells use hydrogenated amorphous silicon (a-Si:H) on crystalline silicon (c-Si) heterojunctions. They provide record efficiencies of 24.7% with front contacts and 25.6% with back contacts thanks to the extremely good passivation of the silicon surface by intrinsic hydrogenated amorphous silicon ((i) a-Si:H) layers and to the high band-gap of a-Si:H [1]. The amorphous nature of a-Si:H leads to a low conductivity and high recombination rate of electron-holes pairs that are generated in the emitter, which limits the conversion of light at short wavelengths.[2,3] To leverage the progresses made in heterojunction solar cells while overcoming these limitations, it would be interesting to integrate new materials as front emitter, with a higher transparency, higher conductivity, and lower recombination rate.

Crystalline materials could be good candidates to meet these criteria. Gallium Phosphide (GaP) has ~0.01% of lattice mismatch with Si and can therefore grow by epitaxy on silicon. Its large bandgap energy of 2.26 eV at 300 K makes it more transparent in the UV than a-Si:H and promises good passivation properties. [4,5,6,7]

Heterojunctions with GaP as the front emitter or as a window layer on silicon solar cells have already been reported.[4,5,6,8,9] However, none of the structures proposed in the literature investigate heterojunction solar cells with a very thin emitter (less than 20 nm) as currently used for a-Si:H / c-Si heterojunctions.

In this paper, we propose to replace the a-Si:H layer by GaP on the front side of heterojunction silicon solar cells. A 5 to 20 nm-thick layer of GaP is grown by epitaxy on nominal <100> silicon by Metal Organic Chemical Vapor Deposition (MOCVD), and the integration flow of a-Si:H/c-Si heterojunction solar cells is used to build a solar cell with a GaP/c-Si heterojunction.

EXPERIMENTAL SETUP

Solar cells are fabricated on p-type ~10 Ω cm <100> double side polished 750 µm-thick 300 mm CZ wafers. After a short 5% HF dip, we coat on an intrinsic a-Si:H film of 5 nm and a n-doped a-Si:H film of 10 nm on the front side. The sample is flipped at the atmosphere and the back side stack consisting of an intrinsic a-Si:H film of

11th International Conference on Concentrator Photovoltaic Systems
AIP Conf. Proc. 1679, 040003-1–040003-5; doi: 10.1063/1.4931514

5 nm and a p-doped a-Si:H film of 10 nm is deposited. A ~70 nm-thick indium tin oxide (ITO) film is deposited on the front side and then on the back side of the sample. Finally, aluminum electrodes are evaporated on each sides of the sample to form a ~400 nm-thick blank sheet at the rear side and a ~400 nm-thick comb electrode on the front side. For the GaP heterostructures, the HF dip and the front side stack deposition are replaced by the GaP deposition process. Before GaP epitaxy, the c-Si surface is deoxidized by a dry process and the crystalline GaP layer with thicknesses between 5 and 20 nm is epitaxially grown. The GaP layer is n-doped by silicon diffusion during the GaP deposition process. Afterward, the samples are dipped in a 5% HF bath and the integration flow continues to deposit the rear side a-Si:H stack and the electrodes.

The GaP epitaxy tool is a molecular organic chemical vapor deposition (MOCVD) tool from Applied Materials developed for microelectronics applications. Amorphous silicon is deposited by Plasma Enhanced Chemical Vapor Deposition (PECVD) and ITO is deposited by Magnetron sputtering. The aluminum is deposited by evaporation. The reflectivity is measured using a Perkin Elmer spectrometer in reflection between 300 nm and 1300 nm with a resolution of 10 nm. The electrical measurements are carried out with a Keithley probe station between -0.5V and 0.5V. The spectral response is determined using a Spequest system. The open circuit voltage is measured as a function of the light illumination using a SunVoc from Sinton. An Aescusoft solar simulator is used for *I(V)* curves extraction in the dark and at AM 1.5G conditions.

RESULTS

Optical Measurements

One of the advantages of GaP for PV applications lies in its optical properties. GaP is non-absorbent for wavelengths above 540 nm, and its optical index (3.3 at 633 nm) is between the optical indexes of air and silicon.[10] This could enable the use of GaP as an efficient anti-reflective coating (ARC). To verify the ARC capability of GaP, we measured the reflectivity of GaP-coated silicon samples with various GaP thicknesses. As shown Figure 1 and Table 1, the total reflectivity across a spectral range of 300 to 1200 nm normalized by the sun spectrum is decreased by coating a GaP layer compared to bare silicon. Opal2 simulations[11] using the dispersion model from Aspnes and Studna [10] are also plotted Figure 1 and show similar trends, except for a lower reflection below 330 nm and above 1040 nm. The difference in the UV region can reasonably be attributed to little differences between dispersion functions from Aspnes and the integrated material. The bump in reflectivity in the IR region for our measurements corresponds to reflections on the back side of the silicon sample compared to the semi-infinite substrate modeled with Opal2. Based on Opal2 simulations, the optimized thickness for the GaP layer to act as an anti-reflective coating would be around 46 nm.

In our integrated cells, a 70 nm-thick layer of ITO is coated on the GaP layer to provide lateral conductivity and enable the contact between GaP and Al. The bi-layer ITO/GaP is then responsible for the anti-reflection properties. According to Opal2, a reflectivity of less than 10 % can be obtained with thicknesses of 34 nm and 77 nm for GaP and ITO, respectively.

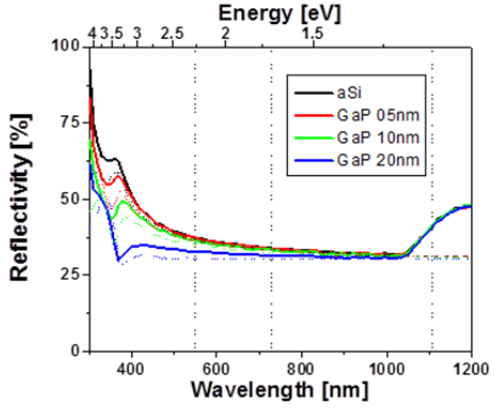

FIGURE 1. Reflectivity of a-Si:H or GaP coated silicon. Plain lines are from measurements while dashed lines are for Opal2 simulations.

TABLE 1. Average reflectivity between 300 and 1300 nm and average reflectivity normalized by the sun spectrum between 300 and 1300 nm for a-Si:H and GaP coated silicon.

	a-Si:H	GaP 05 nm	GaP 10 nm	GaP 20 nm
Reflectivity [%]	40 %	39 %	38 %	35 %
Normalized Reflectivity [%]	38 %	38 %	36 %	33 %

Electrical Measurements

Another advantage of GaP over amorphous silicon is its larger electrical conductivity. According to the literature, GaP resistivity varies between 0.29 and 0.027 Ω.cm for doping level comprised between 5.10^{16} cm^{-3} and more than 10^{19} cm^{-3}.[12] More recent studies have reported a resistivity of 0.02 Ω.cm on thin MOCVD-grown GaP on silicon.[13] In order to determine the conductivity of our structure and the specific contact resistance, we measured the transversal line resistance using the Transmission Line Method (TLM). [14] In all cases, an ohmic contact is obtained and the resistance is extracted from a linear fit of the I(V) curves. The transfer length L_T, sheet resistance R_S of the film and the specific contact resistance ρ_C are reported Table 2.[14] We also report in Table 2 the R_S that would be obtained for a GaP film with a resistivity of 0.027 Ω cm. It is clear that the R_S of our film is 3 to 7 times lower than the calculated values, indicating either a better film quality in our conditions than in previously reported data, a higher doping than expected, or a conduction path in the silicon due to an inversion region.[15] We can notice that the sheet resistance hardly decreases when the thickness increases from 10 to 20 nm. The GaP n-type doping comes from Si diffusion from the substrate which is not optimized yet. Additional measurements using Hall effect estimated the film doping level between 3.10^{18} cm^{-3} and $1.5.10^{19}$ cm^{-3} and the mobility between 200 and 330 $cm^2V^{-1}s^{-1}$ for the GaP thickness of 20 and 5 nm, respectively. However, Hall effect measurements also include electrical conduction from the inversion region at the GaP / c-Si interface and the resulting measurements are rather an effective doping and carrier mobility than actual GaP doping and carrier mobility. Our experimental data tend to indicate that the upper part of the GaP that is less doped than the lower part hardly conducts electricity and that most of the electrical conduction comes from the lower part of GaP that is silicon-doped and from the inversion region in the silicon. The specific contact resistance corresponds to the full contact including aluminum, ITO, GaP and partly the contact resistance between GaP and silicon. We can notice Table 2 that the specific contact resistance increases when the GaP thickness increases. A potential explanation could be the lower doping level at the GaP top surface for the thicker films.

TABLE 2. Transfer length, specific contact resistance and sheet resistance for structures with a-Si:H or GaP. The calculated sheet resistance assumes a resistivity of 0.027 Ωcm for the GaP layer.

	a-Si:H	GaP 5 nm	GaP 10 nm	GaP 20 nm
Transfer length [µm]	123	54	124	189
Contact Resistance [Ω cm^2]	66.5	0.25	0.64	1.46
Measured R_S [Ω/□]	440000	8320	4190	4100
Calculated R_S[Ω/□]		54000	27000	13500

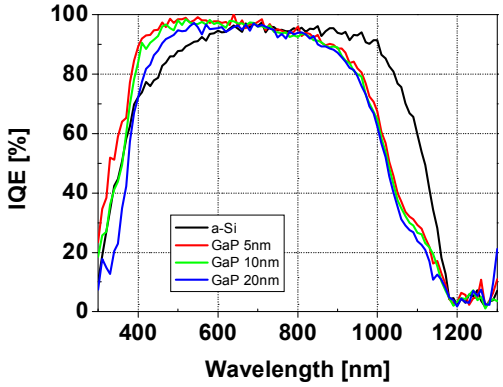

FIGURE 2. Internal Quantum Efficiency (IQE) measured on structures with a-Si:H or GaP with thicknesses of 5, 10 or 20 nm.

Cell Results

Solar cells have been finished using all films investigated here. The cell edges have been isolated by manual scribing and cleaving, resulting in solar cells of approximately 5x5cm^2. These cells have been measured by SunV_{oc}, and I(V) curves have been measured at AM1.5G and in dark conditions. The quantum efficiency has been measured and is reported Figure 2. Table 3 presents the cells results for all samples. The series resistance have been extracted using the one sun and dark I(V) curves as suggested by Dicker.[16,17] We can see that GaP-based solar cells present an efficiency of 7.6, 8.4 and 9% for GaP thicknesses of 20, 10 and 5 nm, respectively. The efficiency is lower than the efficiency of the classical a-Si:H/c-Si solar cell (13.2%). The Internal Quantum Efficiency (IQE) is reported Figure 2. As expected, we can observe in the UV region a strong benefit of the GaP over a-Si:H on the quantum

efficiency since the band gap of GaP is larger than the band gap of s-Si:H. In the IR region (above 800 nm), we observe a degradation of the IQE for the samples with GaP compared to the reference cell. This degradation is explained by the minority carrier lifetime degradation in the silicon during the surface pre-treatment in the MOCVD chamber. This phenomenon has been reported by other groups in the literature [18,19] and was also observed in our conditions. [20]

The lower efficiency for GaP-based solar cells compared to a-Si:H/c-Si heterojunction solar cell has several reasons:

(1) the minority carrier lifetime in the silicon has been degraded during the GaP deposition process. This explains also the lower V_{OC} measured with GaP than with the a-Si:H emitter. This also explains the lower current density that is partially counterbalanced by the lower losses in the UV region (particularly for the thinnest GaP film).

(2) the lower fill factor with GaP based solar cells. The decrease in fill factor is partly attributed to a slightly larger series resistance with GaP, particularly with the larger GaP thickness. We can also notice that for the thinnest GaP layer, the shunt resistance is lower than for a-Si:H, which also reduces the fill factor. This could be explained by conduction paths through the thin GaP. However, the shunt resistance is always larger than 5 kΩ cm^2 and should be large enough for correct cell operation.

It is noticeable that the efficiency of the a-Si:H solar cell is below state of the art heterojunctions a-Si:H/c-Si solar cells which is attributed to the absence of surface texturing, the thickness of the silicon wafer, the un-optimized electrode design and the use of p-type silicon.

TABLE 3. Transfer length, specific contact resistance and sheet resistance for structures with a-Si:H or GaP. The calculated sheet resistance assumes a resistivity of 0.027 Ωcm for the GaP layer.

Sample	V_{OC} [mV]	J_{SC} [mA cm^{-2}]	FF [%]	η [%]	pFF [%]	R_{shunt} [kΩ cm^2]	R_{series} [Ω cm^2]
a-Si:H	654.7	33.2	60.6	13.2	77.9	23	3.2
GaP 5 nm	485.4	34.9	53.1	9.0	79.0	7	4.5
GaP 10 nm	522.1	29.0	55.8	8.4	79.8	370	4.7
GaP 20 nm	525.2	29.5	48.9	7.6	81.2	150	7.0

CONCLUSION

We have evaluated the potential of GaP as a replacement of a-Si:H in heterojunction solar cells. Even if the GaP is more conducting than the a-Si:H, its conductivity is still too low to avoid a transparent conducting electrode for the thicknesses used here. The specific contact resistance increases when the GaP thickness increases, which reduces the fill factor of the cell. The optical response of the cell is improved in the UV region thanks to the lower light absorption of GaP compared to amorphous silicon. With our current process, the surface preparation in the MOCVD chamber degrades the bulk silicon properties and the quantum efficiency for long wavelengths. With the non-optimized process, a cell efficiency of 9% was demonstrated. To improve the cell efficiency, it is compulsory to conserve or improve the minority carrier lifetime in the silicon during the whole deposition process and optimize the structure to reduce the contact resistance.

ACKNOWLEDGEMNTS

The authors acknowledge Pablo Garcia-Linares and Jordi Veirman for fruitful discussions. This work was partly supported by the French RENATECH network. This project has received support from the State Program "Investment for the Future" bearing the reference (ANR -10- ITE -0003).

REFERENCES

1. M. Taguchi, A. Yano, S. Tohoda, K. Matsuyama, Y. Nakamura, T. Nishiwaki, K. Fujita, E. Maruyama, IEEE Journal of Photovoltaics **99**, 1-4 (2013).
2. E. Maruyama, A. Terakawa, M. Taguchi, Y. Yoshimine, D. Ide, T. Baba, M. Shima, H. Sakata, M. Tanaka, Conference Record of the 2006 IEEE 4th World Conference on Photovoltaic Energy Conversion **2**, 1455-1460 (2006).

3. Z. Holman, A. Descoeudres, L. Barraud, F. Fernandez, J. Seif, S. De Wolf, C. Ballif, IEEE Journal of Photovoltaics **2 (1)**, 7-15 (2012).
4. D. L. Feucht, Journal of Vacuum Science and Technology **14 (1)**, 57 (1977).
5. T. Katoda, M. Kishi, J. Electron. Mater. **9 (4)**, 783-796 (1980).
6. G. A. Landis, J. J. Loferski, R. Beaulieu, P. A. Sekula-Moisé, S. M. Vernon, M. B. Spitzer, C. J. Keavney, IEEE Transactions on Electron Devices **37 (2)**, 372-381 (1990).
7. S. A. Ringel, T. J. Grassman, CRC Press Inc, 2010, Ch. 14: III/V Solar Cells on Silicon, pp. 523–576.
8. C. Huang, M. Wang, Z. Deng, Y. Cao, Q. Liu, Z. Huang, Y. Liu, W. Guo, Q. Huang, Semicond. Sci. Technol. **25 (4)**, 045008 (2010).
9. H. Wagner, T. Ohrdes, A. Dastgheib-Shirazi, B. Puthen-Veettil, D. König, P. P. Altermatt, Journal of Applied Physics **115 (4)**, 044508 (2014).
10. D. E. Aspnes, A. A. Studna, Phys. Rev. B **27**, 985–1009 (1983).
11. K. McIntosh, S. Baker-Finch, 38th Photovoltaic Specialists Conference (PVSC), 000265–000271 (2012).
12. H. C. Montgomery, W. L. Feldmann, Journal of Applied Physics **36 (10)**, 3228–3232 (1965).
13. A. Pal, A. Nainani, Z. Ye, X. Bao, E. Sanchez, K. Saraswat, IEEE Transactions on Electron Devices **60 (7)**, 2238-2245 (2013).
14. D. Meier, D. Schroder, IEEE Transactions on Electron Devices **31**, 647 (1984).
15. J.-P. Kleider, J. Alvarez, A. V. Ankudinov, A. S. Gudovskikh, E. V. Gushchina, M. Labrune, O. A. Maslova, W. Favre, M.-E. Gueunier-Farret, P. R. i Cabarrocas, E. I. Terukov, Nanoscale Research Letters **6**, 152 (2011).
16. J. Dicker, "Analyse und Simulation von hocheffizienten Silizium-Solarzellenstrukturen für industrielle Fertigungstechniken", Ph.D. thesis, Universitat Konstanz, 2003.
17. D. Pysch, A. Mette, S. Glunz, Sol. En. Mat. Sol. Cells **91**, 1698-1706 (2007).
18. E. Garcia-Tabares, I. Garcia, J.-F. Lelievre, R.-S. I, Jpn. J. Appl. Phys. **51**, 10ND05 (2012)
19. E. Garcia-Tabares, I. Rey-Stolle, Solar Energy Materials and Solar Cells 124, 17-23 (2014)
20. R. Varache, M. Darnon, M. Descazeaux, T. Quinci, M. Martin, T. Baron, D. Muñoz, 5th International Conference on Silicon Photovoltaics, SiliconPV 2015